Manuscript in press at *Cortex* (March 2021)

Decoding stimuli (tool-hand) and viewpoint invariant grasp-type information

Fredrik Bergström[1, 2], Moritz Wurm[3], Daniela Valério[1, 2], Angelika Lingnau[3, 4] & Jorge Almeida[1, 2]

1. Proaction Laboratory, Faculty of Psychology and Educational Sciences, University of Coimbra, Portugal
2. Faculty of Psychology and Educational Sciences, University of Coimbra, Portugal
3. Center for Mind/ Brain Sciences (CIMeC), University of Trento, 38068 Rovereto (TN), Italy
4. Institute of Psychology, University of Regensburg, 93047 Regensburg, Germany

Corresponding author:

Fredrik Bergström, Faculty of Psychology and Educational Sciences, University of Coimbra, Rua do Colégio Novo, 3001-802 Coimbra, Portugal. e-mail: f.bergstroem@gmail.com

Running title: Decoding stimuli and viewpoint invariant grasp-type

Conflict of interest statement

Declarations of interest: none

Highlights

- Object-directed grasp representations at different levels of abstraction.
- Stimuli (tool-hand) invariant grasps/tool affordances decoded from left PPC.
- Viewpoint invariant grasps decoded from bilateral PPC, left LOTC, and left PMv.

Abstract

When we see a manipulable object (henceforth tool) or a hand performing a grasping movement, our brain is automatically tuned to how that tool can be grasped (i.e., its affordance) or what kind of grasp that hand is performing (e.g., a power or precision grasp). However, it remains unclear where visual information related to tools or hands are transformed into abstract grasp representations. We therefore investigated where different levels of abstractness in grasp information are processed: grasp information that is invariant to the kind of stimuli that elicits it (tool-hand invariance); and grasp information that is hand-specific but viewpoint-invariant (viewpoint invariance). We focused on brain areas activated when viewing both tools and hands, i.e., the posterior parietal cortices (PPC), ventral premotor cortices (PMv), and lateral occipitotemporal cortex/posterior middle temporal cortex (LOTC/pMTG). To test for invariant grasp representations, we presented participants with tool images and grasp videos (from first or third person perspective; 1pp or 3pp) inside an MRI scanner, and cross-decoded power vs. precision grasps across (i) grasp perspectives (viewpoint invariance), (ii) tool images and grasp 1pp videos (tool-hand 1pp invariance), and (iii) tool images and grasp 3pp videos (tool-hand 3pp invariance). Tool-hand 1pp, but not tool-hand 3pp, invariant grasp information was found in left PPC, whereas viewpoint-invariant information was found bilaterally in PPC, left PMv, and left LOTC/pMTG. These findings suggest different levels of abstractness – where visual information is transformed into stimuli-invariant grasp representations/tool affordances in left PPC, and viewpoint invariant but hand-specific grasp representations in the hand network.

Keywords: fMRI, hands, parietal cortex, prehension, tools

1. Introduction

We can immediately and effortlessly recognize how to appropriately grasp any manipulable object (henceforth tool) in our environment (e.g., with a power grasp for a hammer or a precision grasp for a pencil), or what kind of grasping movement our own or someone else's hand is performing (e.g., power or precision grasp). That is because when we see a tool or a hand, our brain automatically infers how that tool can be grasped (i.e., the tool's affordance; Grèzes, Tucker, Armony, Ellis, & Passingham, 2003; Masson, Bub, & Breuer, 2011; Tucker & Ellis, 1998), or what kind of grasp posture that hand has (Bracci, Caramazza, & Peelen, 2018), from the visual information entering our retinae. However, for us to be able to recognize a specific grasp-type across different stimuli, viewpoints, and/or distances despite very different retinal input patterns, the grasp representations must be invariant to the visual features. It is therefore necessary for the brain to process grasp representations at different levels of abstractness by transforming lower-level visual information into invariant (e.g., stimuli or viewpoint invariant) grasp representations. However, it remains unclear where in the human brain such transformations take place. Here we therefore used cross-decoding to investigate where we could find stimulus (tool-hand) and viewpoint-invariant grasp information.

Since invariant grasp representations are activated by both hands and tools separately, they are likely located in one of the brain areas that are activated by observing both hands and tools, i.e., posterior parietal cortices (PPC; centered around the anterior intraparietal sulcus [aIPS], including the anterior part of the inferior parietal lobules [IPL], superior parietal lobules [SPL], and the somatosensory area), posterior middle temporal gyri/lateral occipitotemporal cortex (LOTC/pMTG), and ventral premotor cortices (PMv) (for tools see Almeida et al., 2017; Chao, Haxby, & Martin, 1999; Garcea, Kristensen, Almeida, & Mahon, 2016; Ishibashi, Pobric,

Saito, & Lambon Ralph, 2016; Lee, Mahon, & Almeida, 2019; Lewis, 2006; Mahon et al., 2007; Ruttorf, Kristensen, Schad, & Almeida, 2019); for hands see: Bracci, Cavina-Pratesi, Ietswaart, Caramazza, & Peelen, 2012; Bracci, Ietswaart, Peelen, & Cavina-Pratesi, 2010; Bracci & Peelen, 2013). Consistently, these tool-hand overlap regions seem to represent functional tool-hand interactions (Bracci, Cavina-Pratesi, Connolly, & Ietswaart, 2016; Bracci & Op de Beeck, 2016; Bracci & Peelen, 2013), and are recruited during observed, planned, and executed grasp actions and tool use in humans and non-human primates (Castiello, 2005; Gallivan & Culham, 2015; Gallivan & Goodale, 2018; Ishibashi et al., 2016; Johnson-Frey, 2004; Lewis, 2006).

In non-human primates, visual-motor neurons coding for observed and executed grasp actions have been reported in ventral premotor area F5 (of which a small subset also code for viewpoint invariant grasps; Caggiano et al., 2011) and in PPC (Baumann, Fluet, & Scherberger, 2009; Murata et al., 1997; Murata, Gallese, Luppino, Kaseda, & Sakata, 2000; Raos, Umiltá, Murata, Fogassi, & Gallese, 2006; Schaffelhofer, Agudelo-Toro, & Scherberger, 2015; Taira, Mine, Georgopoulos, Murata, & Sakata, 1990). In humans, however, observed grasp actions recruit LOTC/pMTG in addition to PPC and PMv (Caspers, Zilles, Laird, & Eickhoff, 2010). Consistently, viewpoint-invariant hand information have been found in human left LOTC/pMTG (Bracci et al., 2018), and visual-motor information in LOTC/pMTG and PPC (Oosterhof, Tipper, & Downing, 2012). We therefore expect to be able to decode viewpoint-invariant grasp information from PPC, PMv, and LOTC/pMTG.

In addition to motor-dominant and visual-motor neurons, monkey PPC have visual-dominant neurons that code for visual three-dimensional object properties (Baumann et al., 2009; Murata et al., 1997, 2000; Raos et al., 2006; Sakata, Taira, Kusunoki, Murata, & Tanaka, 1997; Schaffelhofer & Scherberger, 2016; Taira et al., 1990). This makes the monkey, and by extension human, PPC a likely area for visual information to be transformed into invariant grasp

representations. In humans, the left PPC plays a particularly important role for tool-related grasp processing (Buchwald, Przybylski, & Króliczak, 2018; Ogawa & Imai, 2016; Orban, 2016; Orban & Caruana, 2014; Peeters, Rizzolatti, & Orban, 2013), and we therefore expect to be able to decode stimulus (tool-hand) invariant representations from left PPC. Nevertheless, since differences between power and precision grasps have been found in all neural overlap areas during action planning and/or execution (Ariani, Wurm, & Lingnau, 2015; Begliomini, Wall, Smith, & Castiello, 2007; Buchwald, Przybylski, & Króliczak, 2018; Cavina-Pratesi et al., 2018; Di Bono, Begliomini, Castiello, & Zorzi, 2015; Fabbri, Strnad, Caramazza, & Lingnau, 2014; Ogawa & Imai, 2016), we decided to test for stimuli invariance in all overlap areas.

Taken together, the previous literature demonstrates that brain areas with tool- and hand-related neural overlap (i.e., PPC, PMv, and LOTC/pMTG) are associated with observed, planned, and executed grasp actions and tool use. However, it remains unclear to what extent these areas process stimuli (tool-hand) invariant and/or viewpoint-invariant grasp representations. To test this, we presented participants with tool images and grasp videos from first (1pp) or third (3pp) person perspectives in an fMRI scanner, and used cross-classification to decode power vs. precision grasps across (i) viewpoints (viewpoint invariance), (ii) across tool images and grasp 1pp videos (tool-hand 1pp invariance), and (iii) across tool images and grasp 3pp videos (tool-hand 3pp invariance). We found tool-hand (1pp) invariant grasp information in left PPC, and viewpoint-invariant grasp information in bilateral PPC, left PMv, and left LOTC/pMTG, suggesting different levels of grasp-related abstractness.

2. Materials and Methods

Materials and data are available at https://doi.org/10.17605/OSF.IO/4ZF7P.

2.1. Participants

Sixteen participants (M = 21 years, SD = 4.7, 12 females) were recruited from the Faculty of Psychology and Educational Sciences of the University of Coimbra. Sample size was based on previous studies with similar techniques (e.g., Gallivan, Adam McLean, et al. 2013; Chen, Garcea, and Mahon 2016; Gallivan et al. 2016; Ogawa and Imai 2016; Chen et al. 2018). This study was not pre-registered. All exclusion criteria (head motion exceeding voxel size 3 mm; strong scanner artifacts/distortions present) were established prior to data analysis, and we report all manipulations and measures in the study. Due to excessive head motion and/or scanner artifacts, we excluded data from all runs for one (female) participant, from the last three runs for one participant, and from the last two runs for another participant. Thus, 15 participants were used for statistical analyses. All participants had normal or corrected to normal vision, were right handed, gave written informed consent, and received course credits for their participation. The study adhered to the Declaration of Helsinki and was approved by the Ethical Committee of the Faculty of Psychology and Educational Sciences at the University of Coimbra.

2.3. Stimuli and procedure

The study consisted of a localizer experiment (6 runs with a total of 546 volumes per participant) and a main experiment (13 runs across two sessions with a total of 2535 volumes per participant). Stimulus delivery and response collection was controlled using "A Simple Framework" (Schwarzbach, 2011) based on the Psychophysics Toolbox in Matlab R2014a (The MathWorks Inc., Natick, MA, USA). Stimuli were presented on an Avotec projector with a refresh rate of 60 Hz, and viewed by the participants through a mirror attached to the head coil inside the bore of the MR scanner.

For the localizer experiment we used a blocked design, where participants passively viewed grey-scaled images (400 x 400 pixel-size) of tools, hands, animals, famous places, and phase-scrambled versions of each object category. Each object category was pseudo-randomly

presented block-wise (with 12 consecutive images á 500 ms) twice per run, each phase-scrambled object category was presented once per run, each block was separated by 6 s fixation periods, and each run began and ended with a 16 s fixation period (adapted from Fintzi & Mahon, 2014; see also Almeida et al., 2017; Lee et al., 2019). Thus, each object category condition used 12 blocks in total for the univariate analyses.

In the main experiment, we used a mixed design (Figure 1A). During each run, participants were pseudo-randomly presented with two blocks of grey-scaled static (power or precision) tool images, two blocks of grey-scaled (power or precision) grasp videos filmed from a first-person perspective (1pp), and two blocks of grasp videos filmed from a third-person perspective (3pp). Each run began and ended with a 10 s fixation period, and the blocks were separated by 8 s fixation periods throughout each run. The tool-image blocks contained a random mix of 16 tools, out of which eight required a power and eight required a precision grasp when used. Moreover, each block per run had a different set of tool exemplars, totaling 32 different tool images per run (see Figure S1 for all tool images). Similarly, the grasp-video blocks contained a random mix of 16 videos with eight videos where the hand performed a power grasp and eight where a precision grasp was performed. A female and male actor was used to create two equal sets of exemplar grasp videos recorded from 1pp and 3pp. First and third person grasp videos were recorded at the same time, and thus depicted the same exact grasp from different viewpoints. In all videos, the hand started on the table, moved up to perform a tool-specific grasp mid-air, and was then put down on the table. The tool-specific grasps depicted the typical grasps for using those tools (e.g., palmar grasp for a hammer), but were not pantomiming tool use (i.e., not hammering a nail). Thus, every single grasp was uniquely matched to the size and shape of its target tool. Importantly, participants were not told that each grasp video matched the appropriate grasp of a specific tool presented in the tool-image blocks. Instead, the participants were

instructed to press a button whenever they detected a catch trial (i.e., tool chimeras in tool blocks or non-grasping hand movements in grasp-video blocks) that was presented randomly two times in each block. The tool chimeras consisted of a combination of two tools, and the non-grasping movements consisted of a rotating hand with an open palm. The purpose of this task was to keep participants awake while attending to all stimuli. Each block therefore contained 18 trials with 1.5 s stimuli presentations (eight power, eight precision, and two catch trials) separated by 1.5 s fixation periods for a 54 s block duration. In sum, each of the six tool/grasp conditions was repeated 16 times for each of the 13 runs (208 in total), and after removing false alarm trials (i.e., when participants incorrectly pressed the button), there was on average 15.9 (SE = 0.02) repetitions of each tool/grasp condition per run that was used to create run-wise beta maps for the multivariate analysis.

2.4 MRI acquisition

MRI data were collected with a 3T MAGNETOM Trio whole body MR scanner (Siemens Healthineers, Erlangen, Germany) with a 32-channel receive-only head coil across two sessions (one structural run, six localizer runs, five runs for the main experiment in the first session, and eight runs for the main experiment in the second session). The interval between sessions varied from a few days up to four weeks. Structural MRI data were acquired using a T1-weighted magnetization prepared rapid gradient echo (MPRAGE) sequence (repetition time (TR) = 1900 ms, echo time (TE) = 2.32 ms, slice thickness = 0.9 mm, flip angle = 9 degrees, field of view (FoV) = 256 x 256, matrix size = 256 x 256, bandwidth (BW) = 200 Hz/px, GRAPPA acceleration factor 2). Functional MRI (fMRI) data were acquired using a T2*-weighted gradient echo planar imaging (EPI) sequence (TR = 2000 ms, TE = 22 ms, slice thickness = 2.3, FoV = 256 x 256, matrix size = 96 x 96, flip angle = 90 degrees, BW = 1578 Hz/px, GRAPPA acceleration factor 3). Each image volume consisted of 40 contiguous transverse slices recorded

in interleaved slice order oriented parallel to the line connecting the anterior commissure to the posterior commissure covering the whole brain.

2.5. Preprocessing and statistical analysis of fMRI data

2.5.1. Preprocessing

We used SPM12 (Welcome Trust Centre for Neuroimaging, London, UK), run in Matlab R2017b (Mathworks, Inc., Sherborn, MA, USA), for processing and analysis of structural and functional data. Prior to preprocessing, functional volumes were manually inspected for anomalies (e.g., artifacts) with in-house software (DataZ 9D). The structural and functional images were reoriented to approximate MNI space with SPM12 after slice-time correction. The functional data were slice-time corrected to the first slice using a Fourier phase-shift interpolation method. Functional images from both sessions were realigned to the first volume of the first session using 7^{th} degree b-spline interpolation so that all functional images were in the same individual space, and to correct for head motion. Structural images were coregistered to the first functional images. Functional data were normalized to MNI anatomical space using a 12-parameter affine transformation model in DARTEL (Ashburner, 2007), and down-sampled to 3 mm^3 voxel size prior to applying an 8 mm and 3 mm FWHM Gaussian filter for univariate and multivariate analyses, respectively.

2.5.2. Univariate analyses

For within-subject modeling, a General Linear Model (GLM) with restricted maximum likelihood estimation was used. The GLM design matrix for the localizer experiment consisted of 8 regressors of interest (tools, animals, hands, places, and phase scrambled versions of each object category), and head motion (six parameters) as nuisance regressors. All regressors except for head motion were convolved with the "canonical" hemodynamic response function as defined in SPM12. The high-pass filter had a cut-off at 256 s, and the autocorrelation model was global

AR (1). Model estimations from each participant were taken into second-level random-effects analyses (one-sample t-tests) to account for inter-individual variability, and used to define regions of interest for the multivariate analysis.

2.5.3. Regions of interest definitions

A univariate conjunction contrast (hands > animals ∩ tools > animals; Figure 2) was used to identify group and individual peak-coordinates for regions engaged by both hands and tools. We used the conjunction of hands and tools because we wanted to extract shared patterns within the two categories, and assumed the peak conjunction-coordinates would be an optimal starting point. However, for the viewpoint invariant cross-classifications we also used the hand-network (hands > animals) since the viewpoint invariant analysis only contained hands. We used the category animals as baseline because (i) animals are known to engage different areas than hands and tools, and (ii) using another object category instead of phase scrambled images allowed us to focus on high-level category-specific information related to hands and tools. Regions of interest (ROIs) were defined in two steps similar to the steps proposed by (Oosterhof et al., 2012): Firstly, we created group-level spheres with 12 mm radius (with MarsBaR; Brett, Anton, Valabregue, & Poline, 2002) centered on the group's univariate peak-voxel coordinates. Secondly, we created individual-level spheres with 15 mm radius centered on each individual's univariate peak-voxel coordinates but within the group-level spheres (Figure 2). To test how stable effects are across ROI size, we additionally created individual-level spheres with 12 mm radius (Figure S2). All ROIs were defined based on the localizer experiment to avoid circularity, used to extract the individually most relevant beta values from the main experiment to account for individual variability in anatomy, and used for the multivariate analysis. To control for low-level motion or other visual similarities between the two grasp perspectives, we used anatomically defined V1

and V5/MT regions (Jülich SPM Anatomy Toolbox v.3.0; Eickhoff, Heim, Zilles, & Amunts, 2006; Eickhoff et al., 2007, 2005).

2.5.4. Multivariate classification analyses

The GLM design matrix for the main experiment consisted of 8 regressors of interest (power tools, precision tools, power grasps 1pp, precision grasps 1pp, power grasps 3pp, precision grasps 3pp, catch tools, catch grasps), and head motion (six parameters) as nuisance regressors. For each experimental condition, both blocks were used to estimate beta values, which resulted in one beta map per condition per run (i.e., 13 beta maps per condition per participant). The software used for multivariate analysis of the fMRI data was CoSMoMVPA (Oosterhof, Connolly, & Haxby, 2016). The multivariate classification analyses used a leave-one-run-out cross-validation procedure to train a linear discriminant analysis (LDA) classifier to discriminate between z-score normalized beta patterns of two experimental conditions. We estimated each voxel's z-score (across runs) on the training data, and applied the parameters to the test data to remove noise, and thus improve cross-classification performance (Misaki, Kim, Bandettini, & Kriegeskorte, 2010), while keeping training and testing data independent. We used an LDA classifier with shrinkage because it has performed favorably compared to other classifiers when used on visual object information (Mandelkow, de Zwart, & Duyn, 2016; Misaki et al., 2010). The LDA classifier used shrinkage that regularized the matrix by adding the identity matrix scaled by one percent of the mean of the diagonal elements as implemented by CoSMoMVPA Toolbox (Oosterhof et al., 2016; Oosterhof, Wiestler, Downing, & Diedrichsen, 2011). The standard leave-one-run-out cross-validation procedure ensured that training and testing data was kept completely independent. That is, for each iteration in the cross-validation procedure, the training pair from modality A (e.g., a power and precision grasp video) that was in the same run as the testing pair from modality B (e.g., a power and precision tool image) was always omitted. Thus, the LDA

classifier was trained on 11 pairs (omitting one possible training pair) from modality A, and tested on one pair from modality B for each of the 13 cross-validation iterations. More precisely, the LDA classifier was trained to discriminate between power vs. precision within modality A and tested within modality B, then trained on modality B and tested on modality A, and finally averaged across direction for the cross-classification accuracy (Figure 1B).

The group's median classification accuracies were statistically tested with non-parametric Monte Carlo sampling by comparing the probability of each true accuracy to its group level null-distribution with 10,000 null accuracies created by randomly shuffling the condition labels. Condition labels were randomly shuffled within runs prior to running the classification analysis, and iterated 10,000 times per participant to create a participant-by-iterations matrix, from which the median accuracies across participants were used to create a group-level null-distribution. The p-value was computed by counting the number of median accuracies in the null-distribution that were greater than the true median accuracy, divided by the total number of median accuracies in the null-distribution. We used median instead of mean to avoid the group results to be driven by few extreme values, and FDR correction (Benjamini & Hochberg, 1995; Benjamini & Yekutieli, 2001) with a false discovery rate ($q < 0.05$) to correct for multiple comparisons of all tests within each analysis type, i.e., four tests for tool-hand 1pp, four tests for tool-hand 3pp, and ten tests for viewpoint-invariant analyses.

The multivariate searchlight analyses (Kriegeskorte, Goebel, & Bandettini, 2006) used a whole-brain grey-matter mask created by summing each participant's segmented grey matter masks. The searchlight analyses used 15 mm spheres with an LDA classifier with shrinkage to create a mean accuracy map for each participant. The individual accuracy maps for each searchlight analysis were entered into a non-parametric one-sample t-test to obtain group statistics, corrected for multiple comparisons using threshold-free cluster enhanced (Smith &

Nichols, 2009), statistically tested against a Monte Carlo sampled null-distribution created by randomly flipping the signs of the original voxel values for 100,000 iterations, and converting the resulting p-values to z-values as implemented in CoSMoMVPA Toolbox (Oosterhof et al., 2016). There are important differences between the searchlight and ROI analyses to be aware of when interpreting the results. Firstly, the searchlight does not take individual differences in anatomy into account (i.e., each sphere is averaged across individuals at the same spatial position rather than based on individual peak coordinates). Secondly, the searchlight as implemented in CoSMoMVPA statistically tests mean group values rather than median values as used in the ROI analysis. Thirdly, for computational speed, the searchlight permutations randomly flip the signs of the individual accuracies for its non-parametric tests instead of shuffling labels and rerunning the analysis as for the ROI analyses. Fourthly, the searchlight analysis has to correct for more comparisons. These four differences make the searchlight less sensitive than the ROI analyses, which is important to consider when interpreting the differences between searchlight and ROI results.

3. Results

3.1. Behavioral results

The high hit rate (i.e., correctly pressing a button during catch trials; M = 90%, SE = 6%) and low false alarm rate (i.e., mistakenly pressing the button during non-catch trials; M = 0.7%, SE = 0.1%) suggest that participants indeed paid attention to the tool images and grasp videos of interest during the main experiment.

3.2. fMRI results

3.2.1. Univariate localizer results

A localizer experiment was used to pinpoint the tool-hand conjunction and hand peak-coordinates for subsequent multivariate region of interests (ROI) analyses. The conjunction

contrast (hands > animals ∩ tools > animals, FWE $p < 0.05$ cluster corrected) revealed significant BOLD signal change in the left PPC (peak t-value = 8.50, MNI coordinate = [-39 -39 45]; centered around aIPS, and extending across the anterior inferior and superior parietal cortices, and along the posterior border to the secondary somatosensory area), the right PPC (peak t-value = 5.78, MNI coordinate = [39 -42 63]), left LOTC/pMTG (peak t-value = 6.04, MNI coordinate = [-54 -66 -3]), and left PMv (peak t-value = 6.04, MNI coordinate = [-48 6 30]) (Figure 2).

The hands > animals contrast (FWE $p < 0.05$ cluster corrected) showed BOLD signal change in left PPC (peak t-value = 11.67, MNI coordinate = [-36 -39 45]; centered around aIPS, and extending across the anterior inferior and superior parietal cortices, and along the posterior border to the secondary somatosensory area), the right PPC (peak t-value = 9.39, MNI coordinate = [51 -27 42]), left LOTC/pMTG (peak t-value = 11.50, MNI coordinate = [-48 -57 6]), right LOTC/pMTG (peak t-value = 9.91, MNI coordinate = [51 -57 3]), left PMv (peak t-value = 8.53, MNI coordinate = [-48 3 21]), and right PMv (peak t-value = 8.48, MNI coordinate = [54 12 27]).

For completion, the tools > animals contrast (FWE $p < 0.05$ cluster corrected) revealed significant BOLD signal change in the left PPC (peak t-value = 9.44, MNI coordinate = [-39 -39 45]; centered around aIPS, and extending across the anterior inferior and superior parietal cortices to the dorsal occipital cortex, and along the posterior border to the secondary somatosensory area), the right PPC (peak t-value = 6.47, MNI coordinate = [48 -18 36]), left LOTC/pMTG (peak t-value = 6.78, MNI coordinate = [-45 -69 -6]), left PMv (peak t-value = 5.38, MNI coordinate = [-48 6 30]), and left fusiform gyrus (peak t-value = 6.03, MNI coordinate = [-27 -66 12]).

3.2.2. Multivariate classification results

Here we show cross-classification results averaged across directions for more power, but there were no significant differences between directions for any analysis-type or ROI with one

exception (viewpoint invariant, hand-based, left PMv, exact $p = 0.014$; all other ROIs exact $p > 0.066$), and there was no difference between directions for any searchlight analysis.

Regarding hand-tool invariant grasp-specific information in conjunction-based ROIs, we show that neural patterns in left PPC allowed for above chance classification of power vs. precision properties across object categories (i.e., training on tool images and testing on grasp 1pp videos and vice-versa) (Figure 3A). The tool-hand 1pp invariant cross-classification accuracy was significantly higher than chance for left PPC (Mdn = 55.4%, $p = 0.006$, one-tailed), but not for any other ROIs (all $p > 0.246$, one-tailed). The accuracy for left PPC was significantly higher than left LOTC/pMTG (Wilcoxon signed ranks test: $z = 1.97$, exact $p = 0.048$, two-tailed) and left PMv (Wilcoxon signed ranks test: $z = 2.27$, exact $p = 0.021$, two-tailed), but not right PPC (Wilcoxon signed ranks test: $z = 1.70$, exact $p = 0.091$, two-tailed). There were no tool-hand 1pp accuracy differences between other ROIs (all exact $p > 0.309$, two-tailed). Contrarily, the tool-hand 3pp invariant cross-classification accuracies were not above chance in any ROI (all $p > 0.244$, one-tailed), and there were no differences between ROIs (all exact $p > 0.444$, two-tailed). There was no difference between tool-hand 1pp and 3pp accuracies (all exact $p > 0.086$, two-tailed). Taken together, the results show that hand-tool (1pp) invariant grasp-type information was extracted from left PPC.

Regarding viewpoint-invariant grasp-specific information in conjunction-based ROIs, we found that neural patterns from left LOTC/pMTG allowed for classifying power vs. precision grasps across viewpoints (Figure 3A). The viewpoint invariant cross-classification accuracy was significantly higher than chance for left LOTC/pMTG (Mdn = 53.8%, $p = 0.011$, one-tailed), but not for any other ROI (all p between 0.096 and 0.099, one-tailed). There were no viewpoint-invariant accuracy differences between ROIs (all exact $p > 0.303$, two-tailed). However, since viewpoint invariance pertain to hands only, and because Bracci et al. (2018) found that viewpoint

invariance was specific to their hand-based ROI, we tested for viewpoint invariance in all hand-based areas (Figure 3B). The viewpoint invariant accuracy for hand-based ROIs was significantly higher than chance for left PPC (Mdn = 57.7%, p = 0.0001, one-tailed), left LOTC (Mdn = 57.7%, p = 0 [i.e., all 10 000 null permutations were below 57.7%], one-tailed), left PMv (Mdn = 53.8%, p = 0.014, one-tailed), and right PPC (Mdn = 53.8%, p = 0.016, one-tailed), but not in any other ROI (all p > 0.298, one-tailed). There were no viewpoint-invariant accuracy differences between ROIs (all exact p > 0.059, two-tailed). Furthermore, there was no significant differences in viewpoint-invariant accuracy between conjunction- and hand-based ROIs (all exact p > 0.349, two-tailed). Taken together, the results show that viewpoint invariant grasp information was extracted from bilateral PPC, left LOTC, and left PMv.

However, contrary to the tool-hand decoding, the viewpoint invariant decoding could potentially have been influenced by low-level motion or other visual similarities, because both conditions were of identical hands performing identical grasps but from different viewpoints. To control for this possibility, we tried to decode viewpoint invariance from anatomically defined V1 and V5/MT. We were indeed able to decode viewpoint invariance from left V1 (Mdn = 53.8%, p = 0.008) but not from right V1 (Mdn = 50%, p = 0.31), left V5/MT (Mdn = 48.1%, p = 0.72) or right V5/MT (Mdn = 51.9%, p = 0.09), which suggests that there is some low-level similarity between first and third viewpoints that potentially could have influenced the viewpoint invariant decoding.

Lastly, we did a whole-brain searchlight procedure to test for tool-hand (1pp and 3pp) and viewpoint invariant information (Figure 3C). There were no significant clusters of tool-hand (1pp or 3pp) invariant cross-classification after correcting for multiple comparisons (see Figure S3 for uncorrected median accuracy maps). However, a relatively large cluster of viewpoint invariant

cross-classification accuracy was found in left LOTC/pMTG, and a smaller cluster in right middle frontal cortex.

4. Discussion

Tool and hand stimuli have been shown to engage a set of grasp-related regions within the PPC (centered around the aIPS, and including the anterior part of the inferior parietal lobules, superior parietal lobules, and the somatosensory area), left PMv, and left LOTC/pMTG. Here, we investigated whether these regions processed (power or precision) grasp-type information at different levels of abstractness (from hand-specific but viewpoint invariant to stimuli-unspecific hand-tool invariant information). As expected, we found hand-tool invariant grasp-type information in left PPC. However, this was only true when participants observed grasps being performed from first person perspective. In contrast, we found hand-specific but viewpoint-invariant grasp-type information in bilateral PPC, left PMv, and left LOTC/pMTG.

4.1. Tool-hand invariance

We were only able to decode power vs. precision properties across tool images and grasp videos from left PPC. Overall, these results show that at some point in the processing of grasp related information, representations are abstracted away from the visual features of the tools and effectors. According to our data, these representations seem to relate to grasp type (i.e., precision and power grasps), and may serve as a bridge between different effectors and different aspects of tools (perhaps differences in the properties of different exemplars of the same tool) – i.e., between what the system gathers about a tool that constrains the possible functional grasps, and the knowledge of how the effectors may interact with those tools (Sakreida et al., 2016; Valyear, Cavina-Pratesi, Stiglick, & Culham, 2007; Valyear, Gallivan, McLean, & Culham, 2012).

Interestingly, cross-decoding between images of tools and videos of grasps was only observed for those grasps that were shown from a first-person perspective, but not when shown from a third-person perspective. This is consistent with the suggestion that visuospatial information for object-directed actions need to be coded within an egocentric frame of reference, while visual information for object recognition need to be coded within an allocentric frame of reference (Jeannerod, 2001). This may suggest that these tool-hand invariant representations, albeit abstract, pertain to how an individual should act and implement a functional grasp on a target tool, serving as a guide for the interactions between our own effectors and the target tool. One possible conclusion from our data, then, is that at some point in the system, and at a more abstract representational level, processing of first and third person perspectives are separate – that is, processing our own interactions with tools is not equivalent to, or perhaps not even similar to processing someone else's interactions with tools. Alternatively, it could simply be that first person perspectives show stronger effects during relatively passive observation than third person perspectives (but note that paired tests did not reveal a significant accuracy difference between 1pp and 3pp for left PPC).

Our tool-hand invariant finding is consistent with previous literature showing that tool processing is left lateralized in PPC (Almeida, Fintzi, & Mahon, 2013; Almeida et al., 2017; Buchwald et al., 2018; Castiello, 2005; Culham & Valyear, 2006; Gallivan & Culham, 2015; Gallivan & Goodale, 2018; Garcea et al., 2016; Gerbella, Rozzi, & Rizzolatti, 2017; Ishibashi et al., 2016; Jacobs, Danielmeier, & Frey, 2010; Johnson-Frey, 2004; Kristensen, Garcea, Mahon, & Almeida, 2016; Lewis, 2006; Mahon, Kumar, & Almeida, 2013; Rizzolatti & Matelli, 2003; Sakreida et al., 2016; Valyear et al., 2007, 2012). Specifically, it has been shown that left PPC (in particular SMG) is engaged during tool action observation (Peeters et al., 2013; Peeters et al., 2009), contain stable tool affordances (Sakreida et al., 2016), and if damaged produces deficits in

tool use and pantomiming (Almeida et al., 2018; Buxbaum, Kyle, Grossman, & Coslett, 2007; Goldenberg & Hagmann, 1998; Sunderland, Wilkins, Dineen, & Dawson, 2013).

Although some studies have been able to decode grasp-type not only in PPC, but also premotor (Buchwald et al., 2018; Di Bono et al., 2015; Gallivan, McLean, et al., 2013; Turella, Rumiati, & Lingnau, 2020) and LOTC areas (Ariani et al., 2015; Fabbri et al., 2014; Gallivan, McLean, et al., 2013; Turella et al., 2020), their methods differed from ours in important ways. First, they all decoded grasps during action planning and/or execution, while we did so during stimulus observation, which gives our study a greater focus on automatic sensorimotor transformation processes without top-down motor influences. Secondly, some of them decoded grasps more directly without abstracting away from lower-level visual or motor features. Interestingly, two studies that tried to cross-decode invariant grasps across tool-use pantomiming and tool images while thinking about the tool's function (Chen et al., 2018), and tool-use pantomiming across left hand/while seeing tool words and right hand while seeing tool images (Ogawa & Imai, 2016), only found invariant tool-actions in left PPC.

These tool-hand invariant grasp representations are at the top of the dorsal "vision for action" hierarchy, and are likely extracted from stimulus properties analogous to the kinds of neural processes found in monkey PPC. More specifically, invariant grasp representations in human PPC are likely extracted from neurons similar to those found in monkey intraparietal sulcus (AIP) and IPL that are sensitive to visual properties such as object 3D shape, orientation, size, and hand grip (Baumann et al., 2009; Murata et al., 1997, 2000; Raos et al., 2006; Sakata et al., 1997; Schaffelhofer & Scherberger, 2016; Taira et al., 1990), and that code for specific grasp types (Schaffelhofer et al., 2015); while further informed by object texture, weight, and shape from inferotemporal cortex (Almeida et al., 2013; Cavina-Pratesi, Kentridge, Heywood, & Milner, 2010; Gallivan, Cant, Goodale, & Flanagan, 2014; Garcea et al., 2016; Kristensen et al.,

2016; Lee et al., 2019; Lowe, Rajsic, Gallivan, Ferber, & Cant, 2017; Mahon et al., 2013); object identity (Almeida et al., 2013; Almeida, Mahon, & Caramazza, 2010; Mahon et al., 2013), and information related to biological/non-biological motion (Beauchamp, Lee, Haxby, & Martin, 2002), grasping/tool actions (Bracci et al., 2018; Fabbri, Stubbs, Cusack, & Culham, 2016; Gallivan, Chapman, McLean, Flanagan, & Culham, 2013; Gallivan et al., 2015; Gallivan, McLean, et al., 2013; Valyear & Culham, 2010; Vingerhoets & Clauwaert, 2015), and action knowledge (Oosterhof et al., 2012; Vingerhoets, 2008; Wurm & Caramazza, 2019; Wurm & Lingnau, 2015) from left LOTC/pMTG. According to the FARS model, the extracted affordances are then relayed from monkey PCC to F5 (analogous to human PMv), which is responsible for selecting and executing the appropriate grasp (Fagg & Arbib, 1998; Schaffelhofer & Scherberger, 2016). Consistently, we were only able to decode tool-hand invariant representations from left PPC, but not from PMv or left LOTC/pMTG. The lack of tool-hand invariant decoding in PMv could relate to its more prominent role in planning and executing grasps (Gallivan, McLean, et al., 2013; Schaffelhofer & Scherberger, 2016) rather than sensorimotor transformations. The PMv might therefore not be as involved in tasks like ours that relied on observation without motor planning and execution. Although the left LOTC/pMTG has been suggested to process a wide variety of tool and action-related information (for review see Lingnau & Downing, 2015), we were not able to find support for tool-hand invariant information here either. The lack of tool-hand invariant grasp information is similar to Gallivan et al. (2013), who were unable to find cross-effector (tool-hand) information in left LOTC/pMTG, but different from Turella et al. (2020) that found cross-effector (left-right hand) information in LOTC/pMTG. Although it is unclear what underlies this difference, perhaps the invariant information in LOTC/pMTG only is hand-specific, which is consistent with our viewpoint invariant decoding in LOTC/pMTG. However, the precise role of LOTC/pMTG needs further investigation.

4.2. Viewpoint invariance

Additionally, we were able to decode power vs. precision grasp properties across viewpoints in mainly hand-related areas such as bilateral PPC, left PMv, and left LOTC/pMTG, which suggest that shared neural representations within these regions relate to viewpoint-invariant, but hand-specific, grasp information. Being able to extract viewpoint invariant hand posture and movements are necessary for us to understand what a hand is doing (whether grasping or communicating) because the same posture/movement is visually dissimilar from different viewpoints. Our viewpoint invariant findings extend previous findings where viewpoint invariant visual-motor neurons were reported in monkey F5 (Caggiano et al., 2011), visual-motor information within first and third person perspectives separately (across viewpoint was not tested) in human PPC and LOTC/pMTG, and within first person perspective in PMv (Oosterhof et al., 2012), viewpoint-invariant hand-posture information in left LOTC/pMTG (Bracci et al., 2018), and effector-independent information in PPC, PMv, and LOTC/pMTG (Turella et al., 2020). The main reason we found viewpoint invariant representations where others did not could simply be because they did not test the same areas the same way we did. Specifically, Bracci et al. (2018) only performed ROI analysis on left LOTC, Caggiano et al. (2011) only recorded from neurons in PMv, and Oosterhof et al. (2012) only tested within but never across viewpoints. It is possible they would have found the same as us had they performed the same tests in the same regions as us.

Viewpoint invariance in bilateral PPC is a novel finding that likely represents abstract grasp-type information on hand-shape properties that inform the different grasp types, and provide input to cortical areas that focus on motor preparation and execution (e.g., PMv). These hand-shape properties are equivalent but shown from different (first and third person) viewpoints, and may therefore draw upon viewpoint invariant 3D information of these effectors.

Interestingly, the fact that we could decode viewpoint invariant information bilaterally, but tool-hand invariant information only from a first person perspective suggest that at least some action-related properties are not necessarily coded from an egocentric frame of reference. The fact that the viewpoint invariance was bilateral in PPC is interesting because grasping is typically associated with a bilateral activation in aIPS – areas that produce grasping deficits that affects the shaping of the hand when damaged or stimulated (Binkofski et al., 1998; Rice, Tunik, & Grafton, 2006; Tunik, Frey, & Grafton, 2005). This suggests that the viewpoint invariance relates to hand-specific grasp properties in bilateral PPC that is not shared with tool representations, while the tool-hand invariance is left lateralized because it relates specifically to actions with tools. Moreover, Turella et al. (2020) found that bilateral PPC/aIPS contained three levels of abstraction, within effector and orientation, within effector across orientation, and across effector (left-right hand) and orientation, which suggests that PPC might be a central hub for transforming concrete into abstract grasp information.

Viewpoint invariance in human PMv is also a novel finding, which previously only has been shown in visual-motor neurons in monkey F5 (Caggiano et al., 2011). In human PMv, it has only been shown possible to decode hand actions (lift vs. slap) within first person perspective (Oosterhof et al., 2012). This viewpoint invariance might represent more abstract motor programs or action goals and is likely based on information from PPC and LOTC/pMTG. Furthermore, the viewpoint invariance in left LOTC/pMTG is clearly the strongest result as demonstrated by the ROI and whole-brain searchlight, and replicates previous findings (Bracci et al., 2018), and is in line with previous findings that show effector-independent (left-right hand) grasp information in LOTC/pMTG (Turella et al., 2020). The left LOTC/pMTG has been involved in many different action-related tasks, and it is unclear exactly what the viewpoint invariance represents, but it likely relates to a more abstract visual hand shape and/or motion information that is important for

action recognition. The whole-brain searchlight also revealed a small and unexpected cluster in the right middle frontal gyrus, but since it is not an area that has been previously related to hand perception, it is unclear what the significance of this finding is.

Taken together, our viewpoint invariant findings suggest that viewpoint invariant information is processed in several hand-related brain areas associated with action observation (Caspers et al., 2010). We are not able to determine whether this viewpoint invariance is decoded specifically from visual-motor neurons/representations like previous studies, but that is something that can be addressed in future studies.

4.3. Limitations

The viewpoint invariant cross-decoding was derived across hands performing the same grasp movements, and could therefore be confounded by motion similarities or other low-level visual confounds. In our control analysis, we were indeed able to decode viewpoint invariance in left V1 (but not right V1, nor left or right V5/MT), which suggests the presence of some low-level confounds that in principal could have affected the viewpoint invariant results. The viewpoint invariant results should therefore be interpreted with an appropriate amount of caution. However, the control analyses did not show significant effects in V5/MT, which seems to suggest that the viewpoint invariant decoding in left LOTC was not driven by motion similarity. Moreover, the viewpoint invariant decoding in PPC and PMv should not be affected by motion similarity, since those areas are not responsive to low-level motion in the same way as V5/MT. It is unclear exactly what low-level information was decoded in left V1 (or why not right V1), but we think it is unlikely to be driving the viewpoint invariant results.

Importantly, the tool-hand invariant representations were decoded across completely different stimulus material with no discernable similarities in high- or low-level visual features,

or motion similarities since the tool images were static, and should therefore be free of both motion and other low-level visual confounds. However, it might be that the activation of tool-hand invariant grasp representations is modulated by the type of tool stimuli used. For example, using static tool images, tool motion for manipulation, or camera zoom onto tool as if approaching for grasping, could have modulated the classification accuracy in the same or different ROIs. Moreover, using tools that were systematically viewed from first or third person perspectives would have enabled us to further investigate the abstractness of tool-hand invariant representations by comparing classification accuracy for tools and hands from the same viewpoint compared to different viewpoints. However, in this study we wanted to keep things simple to avoid a too complex design manipulation, but it would be interesting to compare different tool stimuli and tool viewpoints in future studies.

For our localizer contrasts we used animals as baseline because we wanted to use a common and relatively neutral object category. It was important to use a common baseline for both tools and hands since we were primarily interested in the conjunction of tools and hands, and using different baselines for tools and hands respectively could have created a bias toward one of them. Importantly, this choice should not have affected ROI localization nor the interpretation of the results, because our tool and hand results match the extensive previous literature where many different object categories (including animals) have been used with consistent results (for tools see Almeida et al., 2017; Chao, Haxby, & Martin, 1999; Garcea, Kristensen, Almeida, & Mahon, 2016; Ishibashi, Pobric, Saito, & Lambon Ralph, 2016; Lee, Mahon, & Almeida, 2019; Lewis, 2006; Mahon et al., 2007; Ruttorf, Kristensen, Schad, & Almeida, 2019); for hands see: Bracci, Cavina-Pratesi, Ietswaart, Caramazza, & Peelen, 2012; Bracci, Ietswaart, Peelen, & Cavina-Pratesi, 2010; Bracci & Peelen, 2013). The peak-voxels we

used would most likely be similar had we used another object category as baseline, and we do therefore not believe that using a different baseline than animals would have changed the outcome.

4.4. Conclusions

In conclusion, our data suggest that visual information is transformed into tool-hand (1pp) invariant grasp-type (power and precision) representations in left PPC, and viewpoint-invariant but hand-specific grasp-type representations in bilateral PPC, left LOTC/pMTG, and left PMv. These invariant grasp representations probably reflect information integration at different levels of processing, where grasps related to tool use might be restricted to left PPC, and hand-specific grasp properties are processed more widely in hand-related areas.

Acknowledgements

This work was supported by Fundação para a Ciência e Tecnologia (PTDC/MHC-PPCN/6805/2014 to J.A., CEECIND/03661/2017 to F.B., SFRH/BD/137737/2018 to D.V.); the European Research Council (Starting Grant number 802553 "ContentMAP" to J.A.); and the German Research Foundation (Heisenberg-Professorship Grant Li 2840/2-1 to A.L.). We thank Lénia Amaral for assisting with stimulus creation, and the Brain Imaging Network Portugal for technical support with the MRI.

References

Almeida, J., Amaral, L., Garcea, F. E., Aguiar de Sousa, D., Xu, S., Mahon, B. Z., & Martins, I. P. (2018). Visual and visuomotor processing of hands and tools as a case study of cross talk between the dorsal and ventral streams. *Cognitive Neuropsychology*, *35*(5–6), 288–303.

https://doi.org/10.1080/02643294.2018.1463980

Almeida, J., Fintzi, A. R., & Mahon, B. Z. (2013). Tool manipulation knowledge is retrieved by way of the ventral visual object processing pathway. *Cortex*, *49*(9), 2334–2344. https://doi.org/10.1016/j.cortex.2013.05.004

Almeida, J., Mahon, B. Z., & Caramazza, A. (2010). The Role of the Dorsal Visual Processing Stream in Tool Identification. *Psychological Science*, *21*(6), 772–778. https://doi.org/10.1177/0956797610371343

Almeida, J., Martins, A. R., Bergström, F., Amaral, L., Freixo, A., Ganho-Ávila, A., … Ruttorf, M. (2017). Polarity-specific transcranial direct current stimulation effects on object-selective neural responses in the inferior parietal lobe. *Cortex*, *94*, 176–181. https://doi.org/10.1016/j.cortex.2017.07.001

Ariani, G., Wurm, M. F., & Lingnau, A. (2015). Decoding Internally and Externally Driven Movement Plans. *Journal of Neuroscience*, *35*(42), 14160–14171. https://doi.org/10.1523/JNEUROSCI.0596-15.2015

Ashburner, J. (2007). A fast diffeomorphic image registration algorithm. *NeuroImage*, *38*(1), 95–113. https://doi.org/10.1016/j.neuroimage.2007.07.007

Baumann, M. A., Fluet, M.-C., & Scherberger, H. (2009). Context-Specific Grasp Movement Representation in the Macaque Anterior Intraparietal Area. *Journal of Neuroscience*, *29*(20), 6436–6448. https://doi.org/10.1523/JNEUROSCI.5479-08.2009

Beauchamp, M. S., Lee, K. E., Haxby, J. V, & Martin, A. (2002). Parallel visual motion processing streams for manipulable objects and human movements. *Neuron*, *34*(1), 149–159. https://doi.org/10.1016/s0896-6273(02)00642-6

Begliomini, C., Wall, M. B., Smith, A. T., & Castiello, U. (2007). Differential cortical activity for precision and whole-hand visually guided grasping in humans. *The European Journal of Neuroscience*, *25*(4), 1245–1252. https://doi.org/10.1111/j.1460-9568.2007.05365.x

Benjamini, Y., & Hochberg, Y. (1995). Controlling the False Discovery Rate : A Practical and Powerful Approach to Multiple Testing. *Journal of the Royal Statistical Society*, *57*(1), 289–300. Retrieved from https://onlinelibrary.wiley.com/doi/10.1002/brb3.412

Binkofski, F., Dohle, C., Posse, S., Stephan, K. M., Hefter, H., Seitz, R. J., & Freund, H. J. (1998). Human anterior intraparietal area subserves prehension: A combined lesion and functional MRI activation study. *Neurology*, *50*(5), 1253–1259. https://doi.org/10.1212/WNL.50.5.1253

Bracci, S., Caramazza, A., & Peelen, M. V. (2018). View-invariant representation of hand postures in the human lateral occipitotemporal cortex. *NeuroImage*, *181*(May), 446–452. https://doi.org/10.1016/j.neuroimage.2018.07.001

Bracci, S., Cavina-Pratesi, C., Connolly, J. D., & Ietswaart, M. (2016). Representational content of occipitotemporal and parietal tool areas. *Neuropsychologia*, *84*, 81–88. https://doi.org/10.1016/j.neuropsychologia.2015.09.001

Bracci, S., Cavina-Pratesi, C., Ietswaart, M., Caramazza, A., & Peelen, M. V. (2012). Closely overlapping responses to tools and hands in left lateral occipitotemporal cortex. *Journal of Neurophysiology*, *107*(5), 1443–1456. https://doi.org/10.1152/jn.00619.2011

Bracci, S., Ietswaart, M., Peelen, M. V, & Cavina-Pratesi, C. (2010). Dissociable neural responses to hands and non-hand body parts in human left extrastriate visual cortex. *Journal of Neurophysiology*, *103*(6), 3389–3397. https://doi.org/10.1152/jn.00215.2010

Bracci, S., & Op de Beeck, H. (2016). Dissociations and Associations between Shape and Category Representations in the Two Visual Pathways. *The Journal of Neuroscience*, *36*(2), 432–444. https://doi.org/10.1523/JNEUROSCI.2314-15.2016

Bracci, S., & Peelen, M. V. (2013). Body and Object Effectors: The Organization of Object Representations in High-Level Visual Cortex Reflects Body-Object Interactions. *Journal of Neuroscience*, *33*(46), 18247–18258. https://doi.org/10.1523/JNEUROSCI.1322-13.2013

Brett, M., Anton, J.-L., Valabregue, R., & Poline, J.-B. (2002). Region of interest analysis using an SPM toolbox [abstract]. *Presented at the 8th International Conference on Functional Mapping of the Human Brain*. Sendai, Japan: Available on CD-ROM in NeuroImage, Vol 16, No 2.

Buchwald, M., Przybylski, Ł., & Króliczak, G. (2018). Decoding Brain States for Planning Functional Grasps of Tools: A Functional Magnetic Resonance Imaging Multivoxel Pattern Analysis Study. *Journal of the International Neuropsychological Society : JINS*, *24*(10), 1013–1025. https://doi.org/10.1017/S1355617718000590

Buxbaum, L. J., Kyle, K., Grossman, M., & Coslett, H. B. (2007). Left inferior parietal representations for skilled hand-object interactions: evidence from stroke and corticobasal degeneration. *Cortex*, *43*(3), 411–423. https://doi.org/10.1016/s0010-9452(08)70466-0

Caggiano, V., Fogassi, L., Rizzolatti, G., Pomper, J. K., Thier, P., Giese, M. A., & Casile, A. (2011). View-based encoding of actions in mirror neurons of area f5 in macaque premotor cortex. *Current Biology : CB*, *21*(2), 144–148. https://doi.org/10.1016/j.cub.2010.12.022

Caspers, S., Zilles, K., Laird, A. R., & Eickhoff, S. B. (2010). ALE meta-analysis of action observation and imitation in the human brain. *NeuroImage*, *50*(3), 1148–1167.

https://doi.org/10.1016/j.neuroimage.2009.12.112

Castiello, U. (2005). The neuroscience of grasping. *Nature Reviews Neuroscience*, *6*(9), 726–736. https://doi.org/10.1038/nrn1744

Cavina-Pratesi, C., Kentridge, R. W., Heywood, C. A., & Milner, A. D. (2010). Separate processing of texture and form in the ventral stream: evidence from FMRI and visual agnosia. *Cerebral Cortex (New York, N.Y. : 1991)*, *20*(2), 433–446. https://doi.org/10.1093/cercor/bhp111

Cavina-Pratesi, Cristiana, Connolly, J. D., Monaco, S., Figley, T. D., Milner, A. D., Schenk, T., & Culham, J. C. (2018). Human neuroimaging reveals the subcomponents of grasping, reaching and pointing actions. *Cortex*, *98*, 128–148. https://doi.org/10.1016/j.cortex.2017.05.018

Chao, L. L., Haxby, J. V., & Martin, A. (1999). Attribute-based neural substrates in temporal cortex for perceiving and knowing about objects. *Nature Neuroscience*, *2*(10), 913–919. https://doi.org/10.1038/13217

Chen, Q., Garcea, F. E., Jacobs, R. A., & Mahon, B. Z. (2018). Abstract Representations of Object-Directed Action in the Left Inferior Parietal Lobule. *Cerebral Cortex*, *28*(6), 2162–2174. https://doi.org/10.1093/cercor/bhx120

Chen, Q., Garcea, F. E., & Mahon, B. Z. (2016). The Representation of Object-Directed Action and Function Knowledge in the Human Brain. *Cerebral Cortex*, *26*(4), 1609–1618. https://doi.org/10.1093/cercor/bhu328

Culham, J. C., & Valyear, K. F. (2006). Human parietal cortex in action. *Current Opinion in Neurobiology*, *16*(2), 205–212. https://doi.org/10.1016/j.conb.2006.03.005

Di Bono, M. G., Begliomini, C., Castiello, U., & Zorzi, M. (2015). Probing the reaching–grasping network in humans through multivoxel pattern decoding. *Brain and Behavior*, *5*(11), 1–18. https://doi.org/10.1002/brb3.412

Eickhoff, S. B., Heim, S., Zilles, K., & Amunts, K. (2006). Testing anatomically specified hypotheses in functional imaging using cytoarchitectonic maps. *NeuroImage*, *32*(2), 570–582. https://doi.org/10.1016/j.neuroimage.2006.04.204

Eickhoff, S. B., Paus, T., Caspers, S., Grosbras, M.-H., Evans, A. C., Zilles, K., & Amunts, K. (2007). Assignment of functional activations to probabilistic cytoarchitectonic areas revisited. *NeuroImage*, *36*(3), 511–521. https://doi.org/10.1016/j.neuroimage.2007.03.060

Eickhoff, S. B., Stephan, K. E., Mohlberg, H., Grefkes, C., Fink, G. R., Amunts, K., & Zilles, K. (2005). A new SPM toolbox for combining probabilistic cytoarchitectonic maps and functional imaging data. *NeuroImage*, *25*(4), 1325–1335. https://doi.org/10.1016/j.neuroimage.2004.12.034

Fabbri, S., Strnad, L., Caramazza, A., & Lingnau, A. (2014). Overlapping representations for grip type and reach direction. *NeuroImage*, *94*, 138–146. https://doi.org/10.1016/j.neuroimage.2014.03.017

Fabbri, S., Stubbs, K. M., Cusack, R., & Culham, J. C. (2016). Disentangling Representations of Object and Grasp Properties in the Human Brain. *Journal of Neuroscience*, *36*(29), 7648–7662. https://doi.org/10.1523/JNEUROSCI.0313-16.2016

Fagg, A. H., & Arbib, M. A. (1998). Modeling parietal–premotor interactions in primate control of grasping. *Neural Networks*, *11*(7–8), 1277–1303. https://doi.org/10.1016/S0893-6080(98)00047-1

Fintzi, A. R., & Mahon, B. Z. (2014). A Bimodal Tuning Curve for Spatial Frequency Across Left and Right Human Orbital Frontal Cortex During Object Recognition. *Cerebral Cortex*, *24*(5), 1311–1318. https://doi.org/10.1093/cercor/bhs419

Gallivan, J. P., Cant, J. S., Goodale, M. A., & Flanagan, J. R. (2014). Representation of Object Weight in Human Ventral Visual Cortex. *Current Biology*, *24*(16), 1866–1873. https://doi.org/10.1016/j.cub.2014.06.046

Gallivan, J. P., Chapman, C. S., McLean, D. A., Flanagan, J. R., & Culham, J. C. (2013). Activity patterns in the category-selective occipitotemporal cortex predict upcoming motor actions. *European Journal of Neuroscience*, *38*(3), 2408–2424. https://doi.org/10.1111/ejn.12215

Gallivan, J. P., & Culham, J. C. (2015). Neural coding within human brain areas involved in actions. *Current Opinion in Neurobiology*, *33*, 141–149. https://doi.org/10.1016/j.conb.2015.03.012

Gallivan, J. P., & Goodale, M. A. (2018). *The dorsal "action" pathway* (H. B. C. Giuseppe Vallar, ed.). https://doi.org/10.1016/B978-0-444-63622-5.00023-1

Gallivan, J. P., Johnsrude, I. S., & Flanagan, J. R. (2015). Planning Ahead: Object-Directed Sequential Actions Decoded from Human Frontoparietal and Occipitotemporal Networks. *Cerebral Cortex*, *26*(2), 708–730. https://doi.org/10.1093/cercor/bhu302

Gallivan, J. P., McLean, D. A., Valyear, K. F., & Culham, J. C. (2013). Decoding the neural mechanisms of human tool use. *ELife*, *2*(2), 1–29. https://doi.org/10.7554/eLife.00425

Garcea, F. E., Kristensen, S., Almeida, J., & Mahon, B. Z. (2016). Resilience to the contralateral visual field bias as a window into object representations. *Cortex*, *81*, 14–23. https://doi.org/10.1016/j.cortex.2016.04.006

Gerbella, M., Rozzi, S., & Rizzolatti, G. (2017). The extended object-grasping network. *Experimental Brain Research*, *235*(10), 2903–2916. https://doi.org/10.1007/s00221-017-5007-3

Goldenberg, G., & Hagmann, S. (1998). Tool use and mechanical problem solving in apraxia. *Neuropsychologia*, *36*(7), 581–589. https://doi.org/10.1016/S0028-3932(97)00165-6

Grèzes, J., Tucker, M., Armony, J., Ellis, R., & Passingham, R. E. (2003). Objects automatically potentiate action: an fMRI study of implicit processing. *European Journal of Neuroscience*, *17*(12), 2735–2740. https://doi.org/10.1046/j.1460-9568.2003.02695.x

Ishibashi, R., Pobric, G., Saito, S., & Lambon Ralph, M. A. (2016). The neural network for tool-related cognition: An activation likelihood estimation meta-analysis of 70 neuroimaging contrasts. *Cognitive Neuropsychology*, *33*(3–4), 241–256. https://doi.org/10.1080/02643294.2016.1188798

Jacobs, S., Danielmeier, C., & Frey, S. H. (2010). Human Anterior Intraparietal and Ventral Premotor Cortices Support Representations of Grasping with the Hand or a Novel Tool. *Journal of Cognitive Neuroscience*, *22*(11), 2594–2608. https://doi.org/10.1162/jocn.2009.21372

Jeannerod, M. (2001). Vision for Action: Neural Mechanisms. In *International Encyclopedia of the Social & Behavioral Sciences* (pp. 16224–16228). https://doi.org/10.1016/B0-08-043076-7/03504-X

Johnson-Frey, S. H. (2004). The neural bases of complex tool use in humans. *Trends in Cognitive Sciences*, *8*(2), 71–78. https://doi.org/10.1016/j.tics.2003.12.002

Kriegeskorte, N., Goebel, R., & Bandettini, P. (2006). Information-based functional brain

mapping. *Proceedings of the National Academy of Sciences*, *103*(10), 3863–3868. https://doi.org/10.1073/pnas.0600244103

Kristensen, S., Garcea, F. E., Mahon, B. Z., & Almeida, J. (2016). Temporal Frequency Tuning Reveals Interactions between the Dorsal and Ventral Visual Streams. *Journal of Cognitive Neuroscience*, *28*(9), 1295–1302. https://doi.org/10.1162/jocn_a_00969

Lee, D., Mahon, B. Z., & Almeida, J. (2019). Action at a distance on object-related ventral temporal representations. *Cortex*, *117*, 157–167. https://doi.org/10.1016/j.cortex.2019.02.018

Lewis, J. W. (2006). Cortical Networks Related to Human Use of Tools. *The Neuroscientist*, *12*(3), 211–231. https://doi.org/10.1177/1073858406288327

Lingnau, A., & Downing, P. E. (2015). The lateral occipitotemporal cortex in action. *Trends in Cognitive Sciences*, *19*(5), 268–277. https://doi.org/10.1016/j.tics.2015.03.006

Lowe, M. X., Rajsic, J., Gallivan, J. P., Ferber, S., & Cant, J. S. (2017). Neural representation of geometry and surface properties in object and scene perception. *NeuroImage*, *157*(June), 586–597. https://doi.org/10.1016/j.neuroimage.2017.06.043

Mahon, B. Z., Kumar, N., & Almeida, J. (2013). Spatial Frequency Tuning Reveals Interactions between the Dorsal and Ventral Visual Systems. *Journal of Cognitive Neuroscience*, *25*(6), 862–871. https://doi.org/10.1162/jocn_a_00370

Mahon, B. Z., Milleville, S. C., Negri, G. A. L., Rumiati, R. I., Caramazza, A., & Martin, A. (2007). Action-Related Properties Shape Object Representations in the Ventral Stream. *Neuron*, *55*(3), 507–520. https://doi.org/10.1016/j.neuron.2007.07.011

Mandelkow, H., de Zwart, J. A., & Duyn, J. H. (2016). Linear Discriminant Analysis Achieves High Classification Accuracy for the BOLD fMRI Response to Naturalistic Movie Stimuli. *Frontiers in Human Neuroscience*, *10*(10), 1283389–128. https://doi.org/10.3389/fnhum.2016.00128

Masson, M. E. J., Bub, D. N., & Breuer, A. T. (2011). Priming of reach and grasp actions by handled objects. *Journal of Experimental Psychology: Human Perception and Performance*, *37*(5), 1470–1484. https://doi.org/10.1037/a0023509

Misaki, M., Kim, Y., Bandettini, P. A., & Kriegeskorte, N. (2010). Comparison of multivariate classifiers and response normalizations for pattern-information fMRI. *NeuroImage*, *53*(1), 103–118. https://doi.org/10.1016/j.neuroimage.2010.05.051

Murata, A., Fadiga, L., Fogassi, L., Gallese, V., Raos, V., & Rizzolatti, G. (1997). Object Representation in the Ventral Premotor Cortex (Area F5) of the Monkey. *Journal of Neurophysiology*, *78*(4), 2226–2230. https://doi.org/10.1152/jn.1997.78.4.2226

Murata, A., Gallese, V., Luppino, G., Kaseda, M., & Sakata, H. (2000). Selectivity for the Shape, Size, and Orientation of Objects for Grasping in Neurons of Monkey Parietal Area AIP. *Journal of Neurophysiology*, *83*(5), 2580–2601. https://doi.org/10.1152/jn.2000.83.5.2580

Ogawa, K., & Imai, F. (2016). Hand-independent representation of tool-use pantomimes in the left anterior intraparietal cortex. *Experimental Brain Research*, *234*(12), 3677–3687. https://doi.org/10.1007/s00221-016-4765-7

Oosterhof, N. N., Connolly, A. C., & Haxby, J. V. (2016). CoSMoMVPA: Multi-Modal Multivariate Pattern Analysis of Neuroimaging Data in Matlab/GNU Octave. *Frontiers in Neuroinformatics*, *10*(July), 047118. https://doi.org/10.3389/fninf.2016.00027

Oosterhof, N. N., Tipper, S. P., & Downing, P. E. (2012). Viewpoint (In)dependence of Action Representations: An MVPA Study. *Journal of Cognitive Neuroscience*, *24*(4), 975–989. https://doi.org/10.1162/jocn_a_00195

Oosterhof, N. N., Wiestler, T., Downing, P. E., & Diedrichsen, J. (2011). A comparison of volume-based and surface-based multi-voxel pattern analysis. *NeuroImage*, *56*(2), 593–600. https://doi.org/10.1016/j.neuroimage.2010.04.270

Orban, G. A. (2016). Functional definitions of parietal areas in human and non-human primates. *Proceedings of the Royal Society B: Biological Sciences*, *283*(1828). https://doi.org/10.1098/rspb.2016.0118

Orban, G. A., & Caruana, F. (2014). The neural basis of human tool use. *Frontiers in Psychology*, *5*(APR), 1–12. https://doi.org/10.3389/fpsyg.2014.00310

Peeters, R. R., Rizzolatti, G., & Orban, G. A. (2013). Functional properties of the left parietal tool use region. *NeuroImage*, *78*, 83–93. https://doi.org/10.1016/j.neuroimage.2013.04.023

Peeters, R., Simone, L., Nelissen, K., Fabbri-Destro, M., Vanduffel, W., Rizzolatti, G., & Orban, G. A. (2009). The Representation of Tool Use in Humans and Monkeys: Common and Uniquely Human Features. *Journal of Neuroscience*, *29*(37), 11523–11539. https://doi.org/10.1523/JNEUROSCI.2040-09.2009

Raos, V., Umiltá, M.-A., Murata, A., Fogassi, L., & Gallese, V. (2006). Functional Properties of Grasping-Related Neurons in the Ventral Premotor Area F5 of the Macaque Monkey. *Journal of Neurophysiology*, *95*(2), 709–729. https://doi.org/10.1152/jn.00463.2005

Rice, N. J., Tunik, E., & Grafton, S. T. (2006). The Anterior Intraparietal Sulcus Mediates Grasp Execution, Independent of Requirement to Update: New Insights from Transcranial

Magnetic Stimulation. *Journal of Neuroscience*, *26*(31), 8176–8182. https://doi.org/10.1523/JNEUROSCI.1641-06.2006

Rizzolatti, G., & Matelli, M. (2003). Two different streams form the dorsal visual system: anatomy and functions. *Experimental Brain Research*, *153*(2), 146–157. https://doi.org/10.1007/s00221-003-1588-0

Ruttorf, M., Kristensen, S., Schad, L. R., & Almeida, J. (2019). Transcranial Direct Current Stimulation Alters Functional Network Structure in Humans: A Graph Theoretical Analysis. *IEEE Transactions on Medical Imaging*, *38*(12), 2829–2837. https://doi.org/10.1109/TMI.2019.2915206

Sakata, H., Taira, M., Kusunoki, M., Murata, A., & Tanaka, Y. (1997). The TINS Lecture. The parietal association cortex in depth perception and visual control of hand action. *Trends in Neurosciences*, *20*(8), 350–357. https://doi.org/10.1016/s0166-2236(97)01067-9

Sakreida, K., Effnert, I., Thill, S., Menz, M. M., Jirak, D., Eickhoff, C. R., … Binkofski, F. (2016). Affordance processing in segregated parieto-frontal dorsal stream sub-pathways. *Neuroscience & Biobehavioral Reviews*, *69*, 89–112. https://doi.org/10.1016/j.neubiorev.2016.07.032

Schaffelhofer, S., Agudelo-Toro, A., & Scherberger, H. (2015). Decoding a Wide Range of Hand Configurations from Macaque Motor, Premotor, and Parietal Cortices. *Journal of Neuroscience*, *35*(3), 1068–1081. https://doi.org/10.1523/JNEUROSCI.3594-14.2015

Schaffelhofer, S., & Scherberger, H. (2016). Object vision to hand action in macaque parietal, premotor, and motor cortices. *ELife*, *5*(JULY). https://doi.org/10.7554/eLife.15278

Schwarzbach, J. (2011). A simple framework (ASF) for behavioral and neuroimaging

experiments based on the psychophysics toolbox for MATLAB. *Behavior Research Methods*, *43*(4), 1194–1201. https://doi.org/10.3758/s13428-011-0106-8

Smith, S. M., & Nichols, T. E. (2009). Threshold-free cluster enhancement: addressing problems of smoothing, threshold dependence and localisation in cluster inference. *NeuroImage*, *44*(1), 83–98. https://doi.org/10.1016/j.neuroimage.2008.03.061

Sunderland, A., Wilkins, L., Dineen, R., & Dawson, S. E. (2013). Tool-use and the left hemisphere: What is lost in ideomotor apraxia? *Brain and Cognition*, *81*(2), 183–192. https://doi.org/10.1016/j.bandc.2012.10.008

Taira, M., Mine, S., Georgopoulos, A. P., Murata, A., & Sakata, H. (1990). Parietal cortex neurons of the monkey related to the visual guidance of hand movement. *Experimental Brain Research*, *83*(1), 29–36. https://doi.org/10.1007/BF00232190

Tucker, M., & Ellis, R. (1998). On the relations between seen objects and components of potential actions. *Journal of Experimental Psychology. Human Perception and Performance*, *24*(3), 830–846. https://doi.org/10.1037//0096-1523.24.3.830

Tunik, E., Frey, S. H., & Grafton, S. T. (2005). Virtual lesions of the anterior intraparietal area disrupt goal-dependent on-line adjustments of grasp. *Nature Neuroscience*, *8*(4), 505–511. https://doi.org/10.1038/nn1430

Turella, L., Rumiati, R., & Lingnau, A. (2020). Hierarchical Action Encoding Within the Human Brain. *Cerebral Cortex*, *30*(5), 2924–2938. https://doi.org/10.1093/cercor/bhz284

Valyear, K. F., Cavina-Pratesi, C., Stiglick, A. J., & Culham, J. C. (2007). Does tool-related fMRI activity within the intraparietal sulcus reflect the plan to grasp? *NeuroImage*, *36*(3), T94–T108. https://doi.org/10.1016/j.neuroimage.2007.03.031

Valyear, K. F., & Culham, J. C. (2010). Observing Learned Object-specific Functional Grasps Preferentially Activates the Ventral Stream. *Journal of Cognitive Neuroscience*, *22*(5), 970–984. https://doi.org/10.1162/jocn.2009.21256

Valyear, K. F., Gallivan, J. P., McLean, D. A., & Culham, J. C. (2012). fMRI Repetition Suppression for Familiar But Not Arbitrary Actions with Tools. *Journal of Neuroscience*, *32*(12), 4247–4259. https://doi.org/10.1523/JNEUROSCI.5270-11.2012

Vingerhoets, G. (2008). Knowing about tools: Neural correlates of tool familiarity and experience. *NeuroImage*, *40*(3), 1380–1391. https://doi.org/10.1016/j.neuroimage.2007.12.058

Vingerhoets, G., & Clauwaert, A. (2015). Functional connectivity associated with hand shape generation: Imitating novel hand postures and pantomiming tool grips challenge different nodes of a shared neural network. *Human Brain Mapping*, *36*(9), 3426–3440. https://doi.org/10.1002/hbm.22853

Wurm, M. F., & Caramazza, A. (2019). Distinct roles of temporal and frontoparietal cortex in representing actions across vision and language. *Nature Communications*, *10*(1), 289. https://doi.org/10.1038/s41467-018-08084-y

Wurm, M. F., & Lingnau, A. (2015). Decoding Actions at Different Levels of Abstraction. *Journal of Neuroscience*, *35*(20), 7727–7735. https://doi.org/10.1523/JNEUROSCI.0188-15.2015

Yekutieli, D., & Benjamini, Y. (2001). The control of the false discovery rate in multiple testing under dependency. *The Annals of Statistics*, *29*(4), 1165–1188. https://doi.org/10.1214/aos/1013699998

Figure captions

Figure 1. Experimental procedure. (**A**) Mixed blocked/event-related experimental design. Each run consisted of two blocks of tool images, grasp videos were presented from a first and third person perspective. Each block included eight power and eight precision tools/grasps, and two chimera/non-grasp catch trials. Each trial consisted of 1.5 s stimulus presentation and 1.5 s fixation presentation. The task was to detect catch trials (i.e., trials consisting of tool chimeras or non-grasping hands). Abbreviations: pow = power trials, pre = precision trials, Ca = catch trials (**B**) A workflow describing the tool-hand (1pp and 3pp) and viewpoint invariant cross-classification analyses with example stimuli from the three conditions with matching power and precision tools and grasps. The LDA classifier is (1) trained to discriminate power vs. precision within one modality and tested on the other modality, (2) trained and tested on the modalities in the reverse order, and (3) averaged across the two directions for the final cross-classification LDA accuracy.

Figure 2. Localizer results. Group-level univariate localizer results showing the conjunction (hands > animals ∩ tools > animals), hands > animals, and tools > animals, FWE $p < 0.05$ cluster corrected). The conjunction contrast and hands > animals contrast were used to find peak-voxel coordinates for the multivariate region of interest analysis. The tools > animals contrast is shown for completion.

Figure 3. Classification results. (**A**) Summation heat map of individual spheres centered on peak voxels from the conjunction contrast, and boxplot graph with conjunction-based cross-classification results. (**B**) Summation heat map of individual spheres centered on peak voxels

from hands > animals contrast, and boxplot graph with hand-based cross-classification results. In the graphs, average (across directions) LDA accuracy is shown on the y-axis, regions of interest on the x-axis, and boxplots show median viewpoint and tool-hand (1pp and 3pp) invariant classification accuracy. The black horizontal line shows chance-level (50%), colored dots indicates outliers, * $p < 0.05$, ** $p \leq 0.01$, *** $p \leq 0.001$, and red * FDR $q \leqslant 0.05$. FDR corrected for all tests within each analysis type (4 x tool-hand 1pp, 4 x tool-hand 3pp, 10 x viewpoint). (**C**) Whole-brain searchlight results for viewpoint invariant cross-classification. The figure shows threshold-free cluster-enhanced z-maps ($z \geq 1.65 = p < 0.05$, one-tailed).

Supplemental material captions

Figure S1. Tool images. All 32 power and precision tool images, and four tool chimera catch images, used in the main experiment.

Figure S2. Classification results. (**A**) Summation heat map of 12 mm individual spheres centered on peak voxels from the conjunction contrast, and boxplot graph with conjunction-based cross-classification results. (**B**) Summation heat map of individual spheres centered on peak voxels from hands > animals contrast, and boxplot graph with hand-based cross-classification results. In the graphs, average (across directions) LDA accuracy is shown on the y-axis, regions of interest on the x-axis, and boxplots show median viewpoint and tool-hand (1pp and 3pp) invariant classification accuracy. The black horizontal line shows chance-level (50%), colored dots indicates outliers, * $p < 0.05$, ** $p \leq 0.01$, *** $p \leq 0.001$, and red * FDR $q \leqslant 0.05$. FDR corrected for all tests within each analysis type (4 x tool-hand 1pp, 4 x tool-hand 3pp, 10 x viewpoint).

Here we show cross-classification results averaged across direction for more power, but there were no significant differences between directions for any analysis-type or ROI with one exception (tool-hand 3pp invariant, left LOTC, exact $p = 0.027$; all other ROIs exact $p > 0.081$). Regarding hand-tool invariant grasp-specific information in conjunction-based ROIs, we show that neural patterns in left PPC allowed for above chance classification of power vs. precision properties across object categories (i.e., tool images and grasp 1pp videos). The tool-hand 1pp invariant cross-classification accuracy was significantly higher than chance for left PPC (Mdn = 53.8%, $p = 0.012$, one-tailed), but not for any other ROIs (all $p > 0.250$, one-tailed). The accuracy for left PPC was not significantly higher than any other ROI (all exact $p > 0.058$, two-tailed). There were no other tool-hand 1pp accuracy differences between ROIs (all exact $p > 0.657$, two-tailed). The tool-hand 3pp invariant cross-classification accuracies were not above chance for any ROI (all $p > 0.700$, one-tailed), and there was no tool-hand 3pp accuracy differences between ROIs (all exact $p > 0.333$, two-tailed). The tool-hand 1pp accuracy for left PPC was higher than the tool-hand 3pp accuracy for left LOTC/pMTG (Wilcoxon signed ranks test: $z = 2.45$, exact $p = 0.012$, two-tailed), but no other differences between tool-hand 1pp and 3pp (all exact $p > 0.064$, two-tailed). Taken together, the results show that hand-tool 1pp invariant grasp-type information was found in left PPC.

Regarding viewpoint-invariant grasp-specific information in conjunction-based ROIs, we found that neural patterns from left and right PPC allowed for classifying power vs. precision grasps across viewpoints. The viewpoint invariant cross-classification accuracy was significantly higher than chance for left PPC (Mdn = 55.4%, $p = 0.0083$, one-tailed) and right PPC (Mdn = 53.8%, $p = 0.010$, one-tailed), but not for any other ROI (all $p > 0.315$, one-tailed). There were no viewpoint-invariant accuracy differences between ROIs (all exact $p > 0.311$, two-tailed). The viewpoint invariant accuracy for hand-based ROIs was significantly higher than chance for left

PMv (Mdn = 53.8%, p = 0.014, one-tailed) and right PMv (Mdn = 53.8%, p = 0.015, one-tailed), but not for any other ROI (all p > 0.068, one-tailed). There were no viewpoint-invariant accuracy differences between ROIs (all exact p > 0.197, two-tailed). Furthermore, there was no significant difference for viewpoint-invariant accuracy between conjunction- and hand-based ROIs (all exact p > 0.293, two-tailed). Taken together, the results show that viewpoint invariant grasp information was extracted from bilateral PPC and bilateral PMv areas.

Figure S3. Searchlight maps. Uncorrected median accuracy searchlight maps. (**A**) Tool-hand (1pp) invariance uncorrected accuracy maps. (**B**) Tool-hand (3pp) invariant uncorrected accuracy maps. Note, these accuracy maps show median values to be more consistent with region of interest analyses, but the searchlight analysis as implemented in CoSMoMVPA Toolbox statistically tested mean values.

Figure1

Click here to access/download;Figure;Figure1.tif

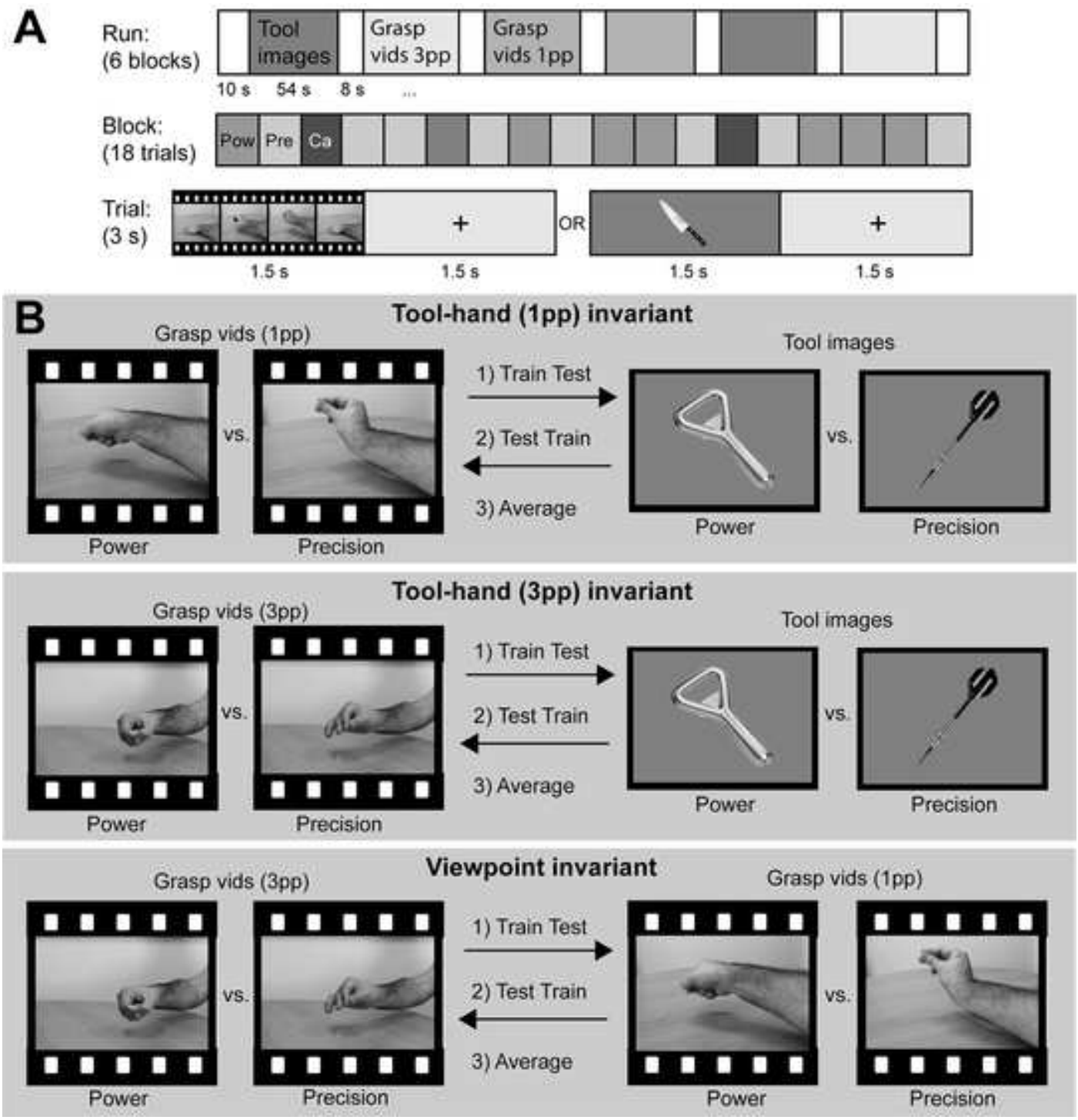

Figure2

Click here to access/download;Figure;Figure2.tif

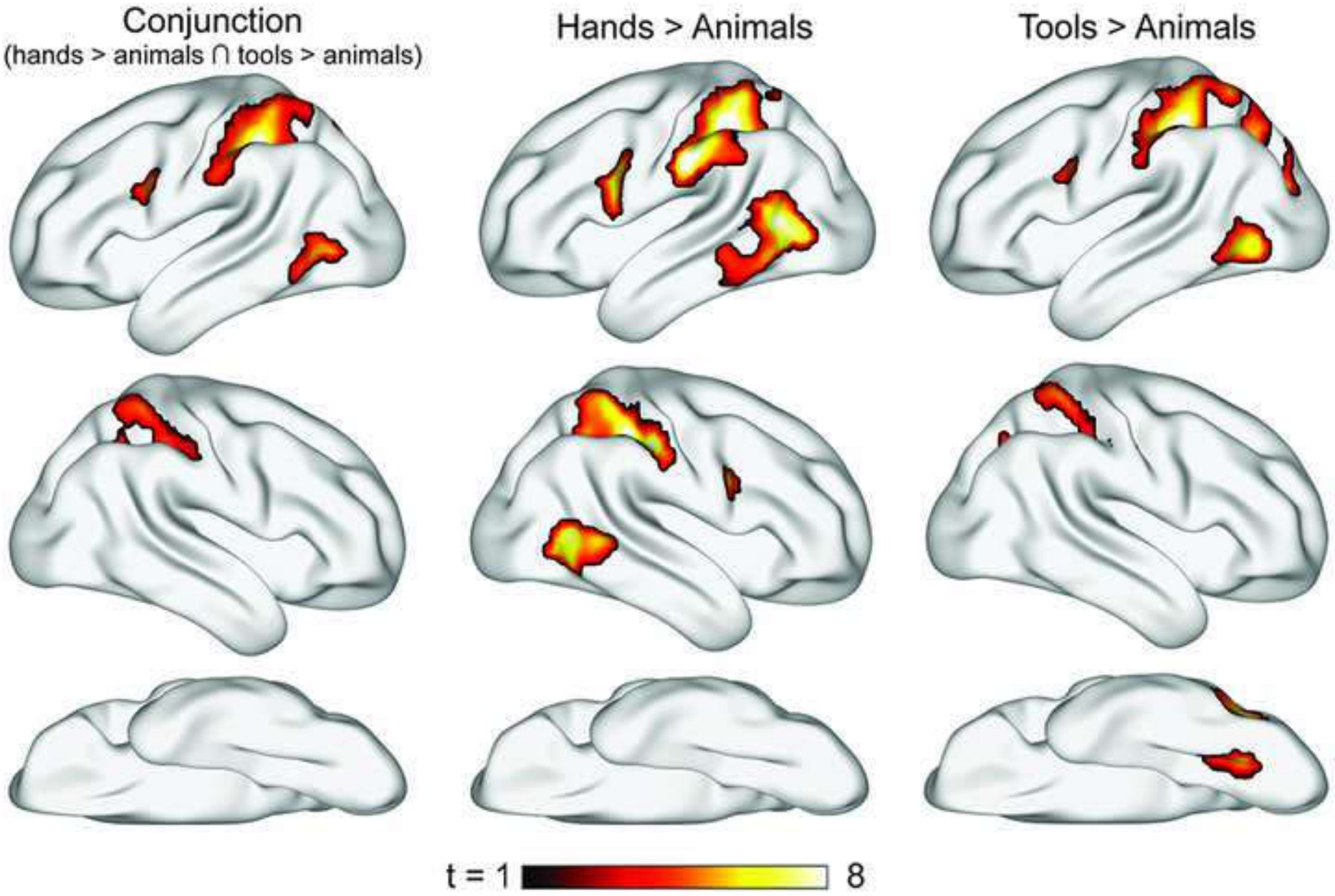

Figure3

Click here to access/download;Figure;Figure3.tif

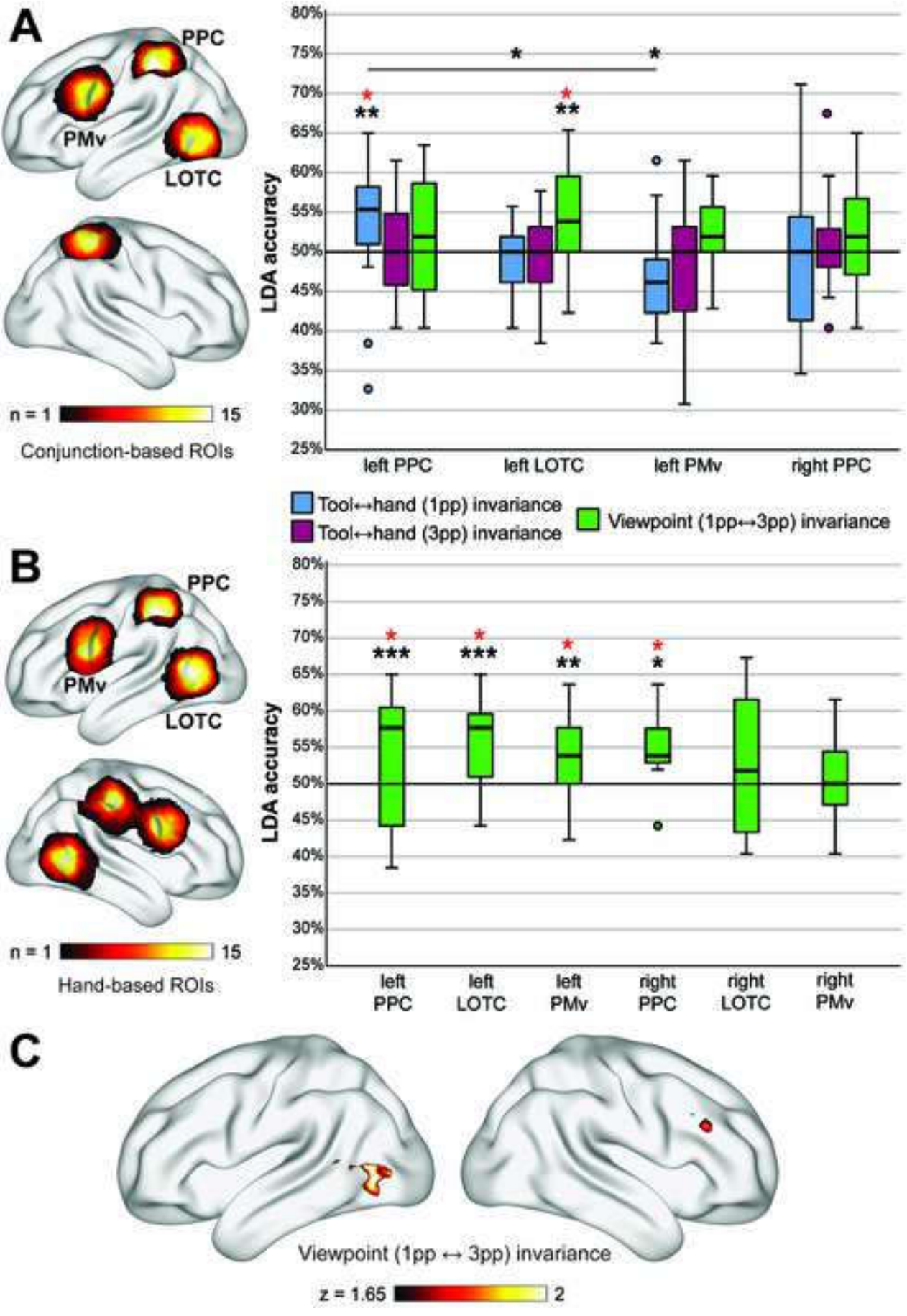

FigureS1

Click here to access/download;Figure;FigureS1.tif

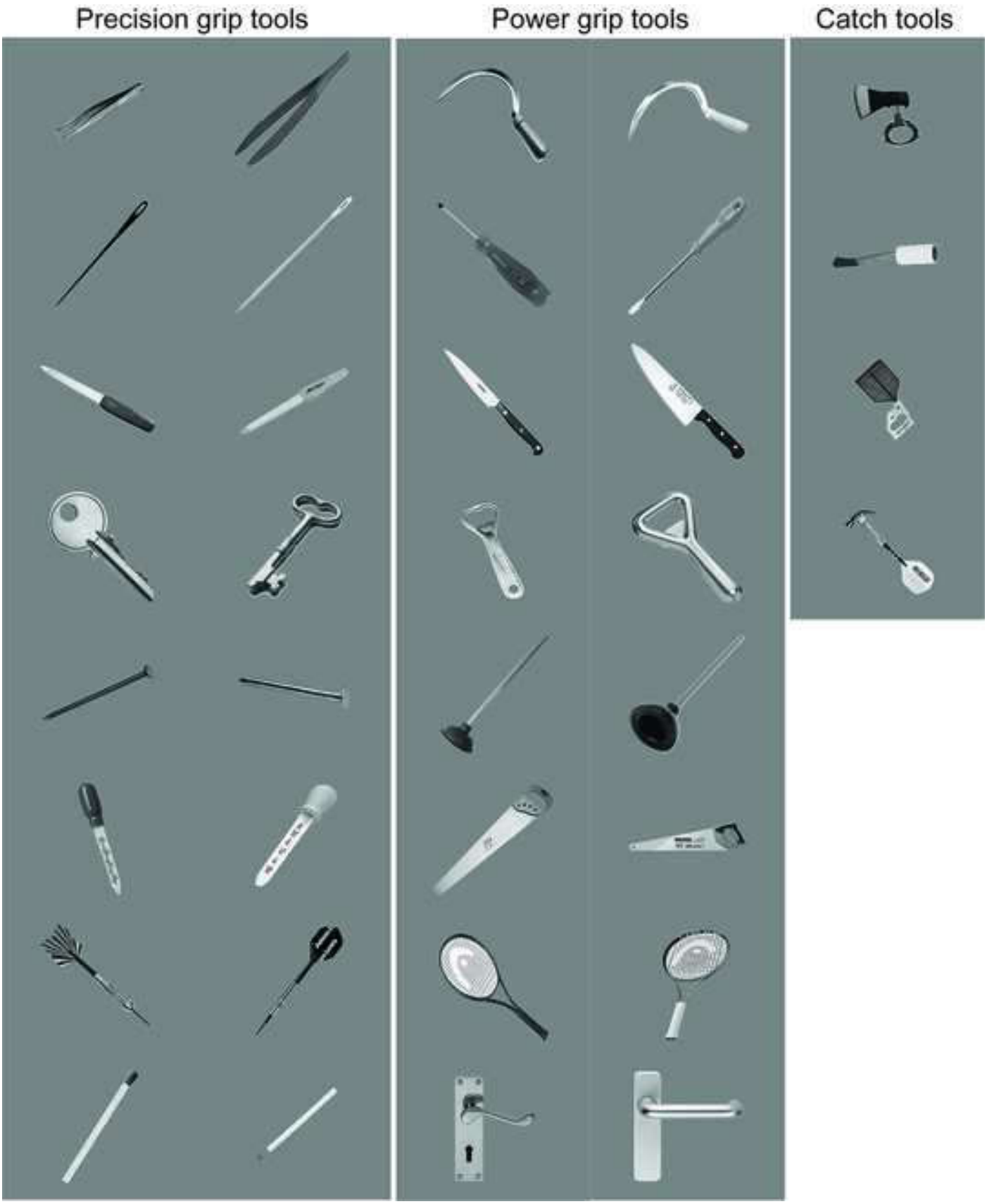

FigureS2

Click here to access/download;Figure;FigureS2_90mm.tif

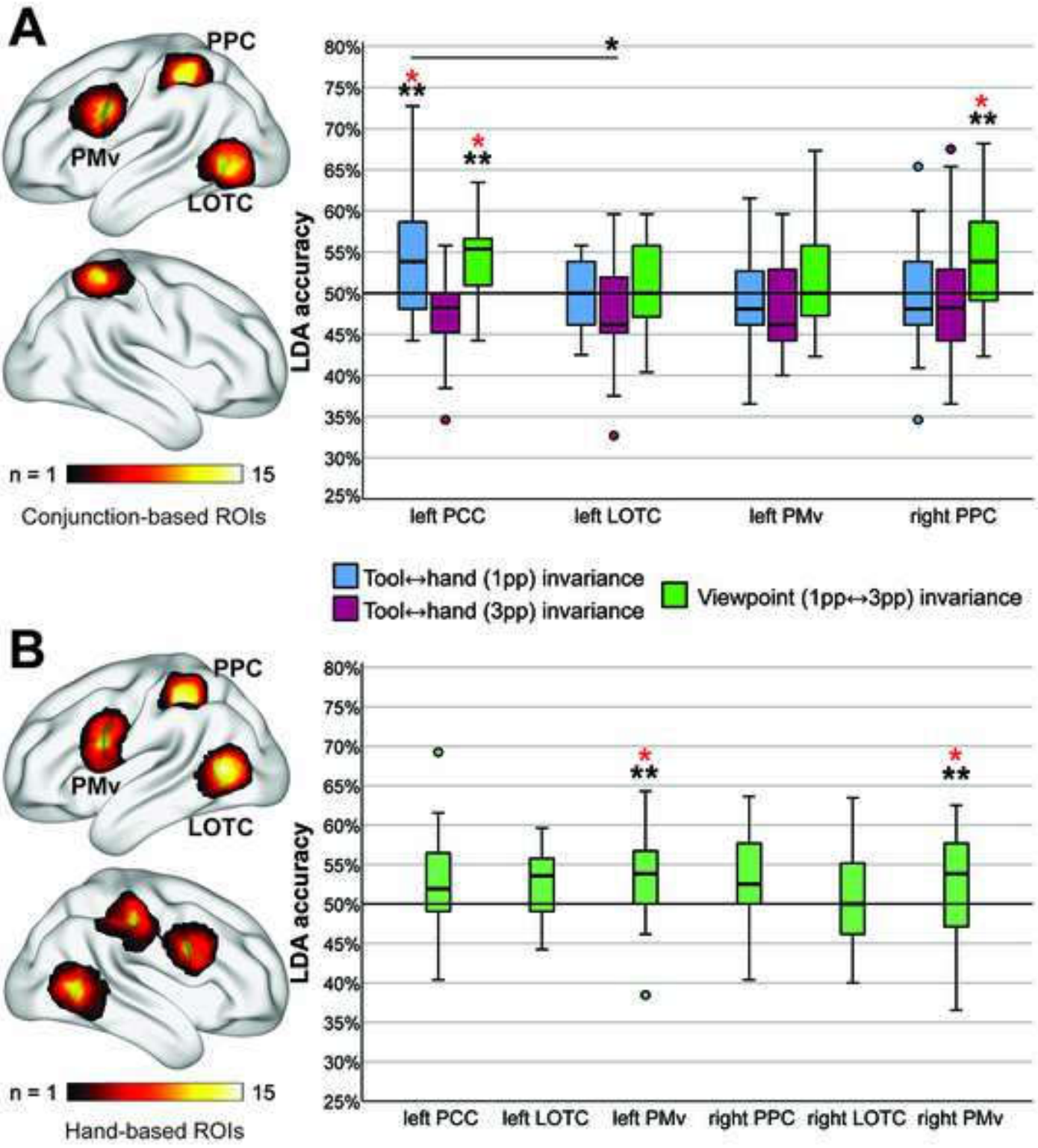

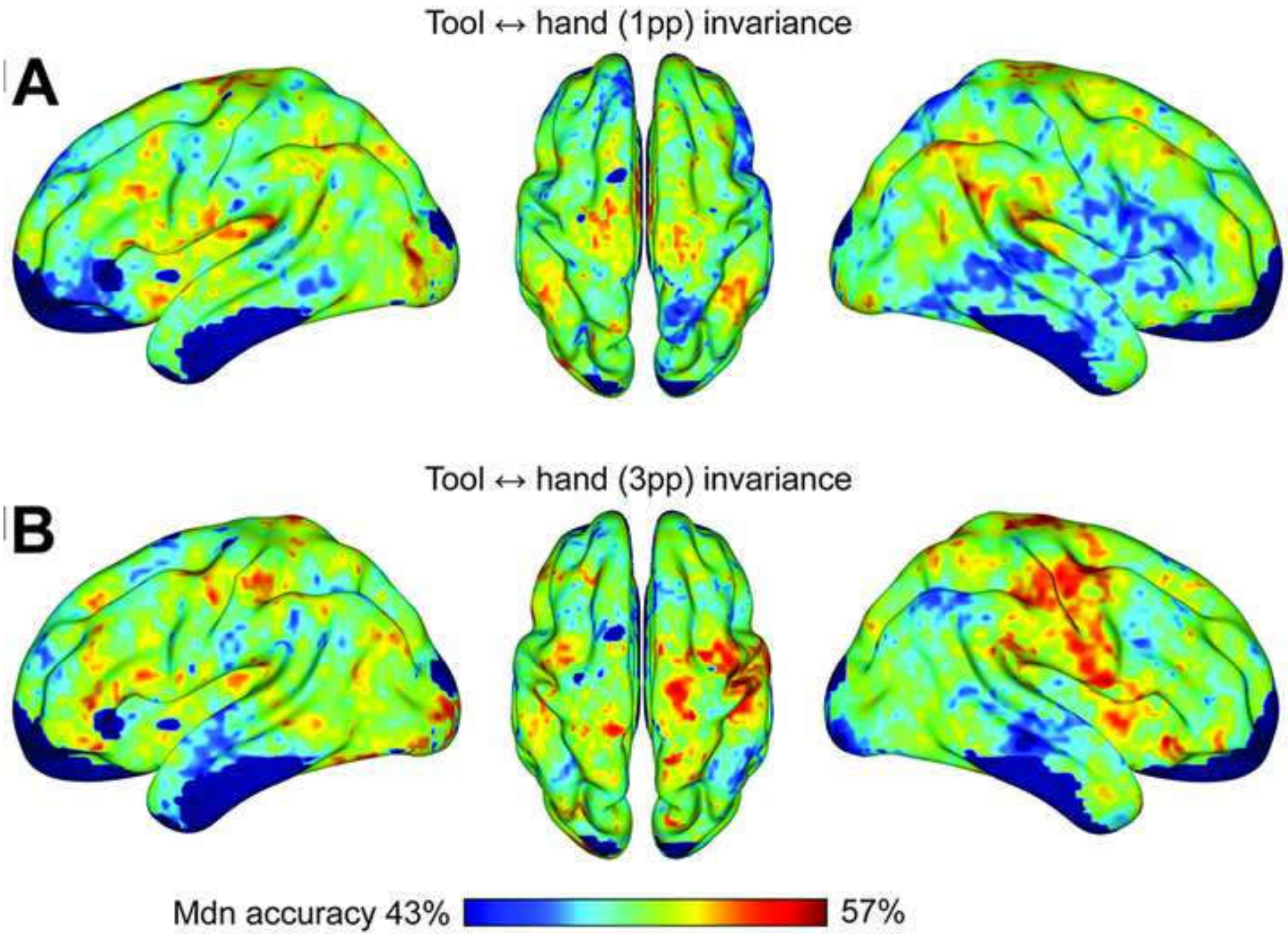

CrediT authorship contribution statement

Fredrik Bergström: Investigation, methodology, data curation, formal analysis, writing – original draft, review & editing.

Moritz Wurm: Conceptualization, methodology, writing – review & editing.

Daniela Valério: Investigation, methodology.

Angelika Lingnau: Conceptualization, methodology, writing – review & editing.

Jorge Almeida: Conceptualization, methodology, data curation, funding acquisition, supervision, writing – review & editing.